Tetrahedron Letters 160 (2025) 155546

Contents lists available at ScienceDirect

Tetrahedron Letters

journal homepage: www.elsevier.com/locate/tetlet

Diversification of acridinium photocatalysts: Property tuning and reactivity in model reactions

Jason Y. Wang [a,1], Flora Fan [a,1], Madeline E. Ruos [a,1], Leticia Adao Gomes [b], Mimi Lavin [a,c], Thomas J. O'Connor [a], Steven A. Lopez [b,*], Abigail G. Doyle [a,*]

[a] Department of Chemistry and Biochemistry, University of California, Los Angeles, CA 90095, United States
[b] Department of Chemistry and Chemical Biology, Northeastern University, Boston, MA 02115, USA
[c] Present address: Department of Chemistry, Columbia University, New York, NY 10027, USA

ARTICLE INFO

Keywords:
Photoredox catalysis
Acridiniums
Excited state lifetime

ABSTRACT

Herein, we describe the discovery and characterization of multiple *N*-(hetero)aryl, *N*-benzyl and *N*-alkyl derivatives of 9-mesityl-3,6-di-*tert*-butyl-10-phenyl acridinium photocatalyst. The catalytic performances of these catalysts as photo-oxidant or photo-reductant (via *in situ* generated acridine radical) were compared in three model reactions. We also identified improved catalytic conditions for a previous cyanoarene-catalyzed nucleophilic amination reaction using a synthesized *N*-cycloheptyl acridinium catalyst (up to 98 % yield).

Introduction

In photoredox catalysis, late transition-metal (e.g., iridium, ruthenium) polypyridyl complexes have been commonly employed as photocatalysts, due to their favorable excited redox properties, enhanced photostability and excited state lifetime. However, the high cost and low abundance of these metals have prompted the discovery and application of organic photocatalysts. Organic photocatalysts (OPCs) usually have extended conjugated systems and absorb visible light to reach excited states that can also engage in photoredox catalysis. 9-mesityl-3,6-di-*tert*-butyl-10-phenyl acridinium salt (**1**) and its derivatives have found applications in synthetic transformations such as nucleophilic arene and alkene functionalization [1]. Modular syntheses that are amenable to late-stage functionalization [2–8] have enabled access to diverse acridinium derivatives. However, studies on the comparison of their catalytic performances under various reduction and oxidation manifolds have been limited. Using **1** as a template structure, we set out to examine the effects of structural changes on the photophysical properties and various reactivities of acridinium photocatalysts.

Underexplored *N*-substitutions for acridinium photocatalysts

Our investigation started by identifying underexplored structural motifs for derivatives of **1**. Prior reports suggested that modifications to the acridinium core do not significantly change the redox potentials of the catalysts (vide infra). On the other hand, modifications to the *N*-substituent, while also having little effect on redox potentials, can lead to meaningful changes in excited state lifetimes. Based on these observations, we synthesized a library of previously unknown catalysts with various *N*-substituents (aryl, heteroaryl, benzyl, alkyl) from xanthylium salts and commercially available amines (Fig. 1b).

We characterized the photophysical properties of the synthesized catalysts (Table 1), focusing on excited-state reduction potential ($E^*_{red} = E_{0,0} + E_{red}$, vs. SCE) and excited-state lifetime (τ). For comparison, we also compiled properties of acridinium catalysts in three prior reports [2,6,8] that can be accessed via the same synthetic procedure. To visualize the effect of structural modifications on E^*_{red} and τ, we also defined a structural difference score. This score is calculated as 1 minus the Tanimoto similarity [9] of RDKit fingerprints [10] for a synthesized catalyst and **1**. The higher the structural difference score, the more different a given catalyst structure is compared to **1**. Both synthesized and reported acridinium catalysts are shown for comparison (Fig. 1c). Compared to **1** ($E^*_{red} = +2.10$ V, $\tau = 13.8$ ns [2]), structural modifications have little impact on E^*_{red} ($\pm$ 0.2 V), while significant changes to excited state lifetimes of over $\pm$10 ns can be observed. Compared to derivatives reported in the literature, our library features simple changes to the *N*-substituents, but covers a broad range of property differences. Notably, we observed increased excited-state lifetimes for a

* Corresponding authors.
E-mail addresses: s.lopez@northeastern.edu (S.A. Lopez), agdoyle@chem.ucla.edu (A.G. Doyle).
[1] Equal contributions

https://doi.org/10.1016/j.tetlet.2025.155546
Received 19 February 2025; Received in revised form 10 March 2025; Accepted 11 March 2025
Available online 22 March 2025

variety of *N*-alkyl and *N*-aryl acridiniums. It has been suggested that a more hindered C—N bond rotation can result in slower nonradiative decay pathways, thus increasing excited-state lifetimes [2]. This hypothesis is further evidenced by the observation that multiple C—N rotamers exist at room temperature (see Supporting Information for NMR studies) for certain acridiniums (**A4**, **A5**, **A8**).

To examine the effect of various *N*-substituents on the excited-state nature of acridinium photocatalysts, we performed time-dependent density functional theory (TD-DFT) calculations on the optimized S_1 geometry of the synthesized acridiniums (see Supporting Information for more details). These calculations indicate electron transitions from the mesityl group or the *N*-substituent to the acridinium core in the excited state. These orbitals have minimal spatial orbital overlap, suggesting that S_1 is an intramolecular charge-transfer (CT) state. We also observed a significant increase in dipole moments from S_0 to S_1 optimized geometries, further supporting the characterization of S_1 as a CT state.

Acridiniums in S_NAr reaction

Established acridinium photocatalysts such as **1** and **2** are often employed as strong excited-state oxidants. Thus, we decided to test our library of novel acridinium photocatalysts under an oxidative manifold, in the S_NAr reaction of anisoles, as reported by Nicewicz and coworkers [13]. Given that the coupling combination of anisole with 1,3-imidazole was reported to occur in a modest 39 % yield with **1**, we were curious to observe how our library of catalysts with modified *N*-substitutions would perform (Fig. 2a). Unsurprisingly, catalyst **A10**, being most structurally and electronically like **1**, enabled the reaction to proceed with similar yields, with low conversion of anisole, likely resulting from slow catalyst turnover with this substrate pairing. Surprisingly, photocatalysts **A4** and **A5** with alkyl substitution performed the next highest out of our acridinium library, though did not outperform **1**.

Thus, we were interested to observe whether we could exploit the significantly longer lifetime of *N*-alkyl substituted acridiniums by lowering the catalyst loading required. We performed a head-to-head comparison between **A5** and **1** in the reaction of imidazole with *ortho*-chloroanisole, which was reported to proceed with high yield. We found that at a decreased 2 mol% catalyst loading, both acridinium photocatalysts performed comparably to each other (Fig. 2b). Although the overall yield was much lower than with the standard reaction conditions, our results imply that the longer excited state lifetime of *N*-alkyl acridinium photocatalysts could potentially be leveraged in other reactions.

It is also worth noting that all our tested acridinium photocatalysts were competent in this reaction. This finding led us to wonder about the significance of the *N*-phenyl substitution in **1**. Therefore, we decided to next screen our library in a different reaction that mechanistically emphasizes its importance (vide infra).

Table 1
Experimentally determined photophysical properties of synthesized acridinium photocatalysts. Detailed characterizations and methods of determination can be found in the Supporting Information section 4. Discussions on multiple excited-state lifetimes observed can also be found in the Supporting Information section 4. E_{red}: ground state reduction potential, or $E_{1/2}(C/C^-)$, vs. SCE; $E_{0,0}$: Excited-state energy; E^*_{red}: excited-state reduction potential, or $E_{1/2}(C^*/C^-)$, vs. SCE; τ: fluorescence lifetime.

Catalyst label	E_{red} (V)	$E_{0,0}$ (eV)	E^*_{red} (V)	τ (ns)
1[a]	−0.56	+2.66	+2.10	13.8
2[b]	−0.49	+2.37	+1.88	6.4
A1	−0.61	+2.64	+2.03	15.09
A2	−0.59	+2.73	+2.14	0.11, 4.41, 15.02
A3	−0.61	+2.64	+2.03	23.52
A4	−0.64	+2.63	+1.99	26.91
A5	−0.63	+2.66	+2.03	23.18
A6	−0.63	+2.67	+2.04	0.15, 4.93, 18.93
A7	−0.45	+2.68	+2.23	0.3, 8.53, 16.85
A8	−0.59	+2.68	+2.09	0.26, 8.85, 18.45
A9	−0.56	+2.66	+2.10	12.38
A10	−0.62	+2.65	+2.03	6.14
A11	−0.56	+2.66	+2.10	12.58

[a] Catalyst properties extracted from [2].
[b] Catalyst properties extracted from [11,12].

Acridiniums in photo-debromination reaction

Nicewicz and coworkers also reported **1** to be a highly competent photocatalyst in a series of dehalogenation reactions, in which the catalyst acts as a super-reductant capable of reducing various aryl

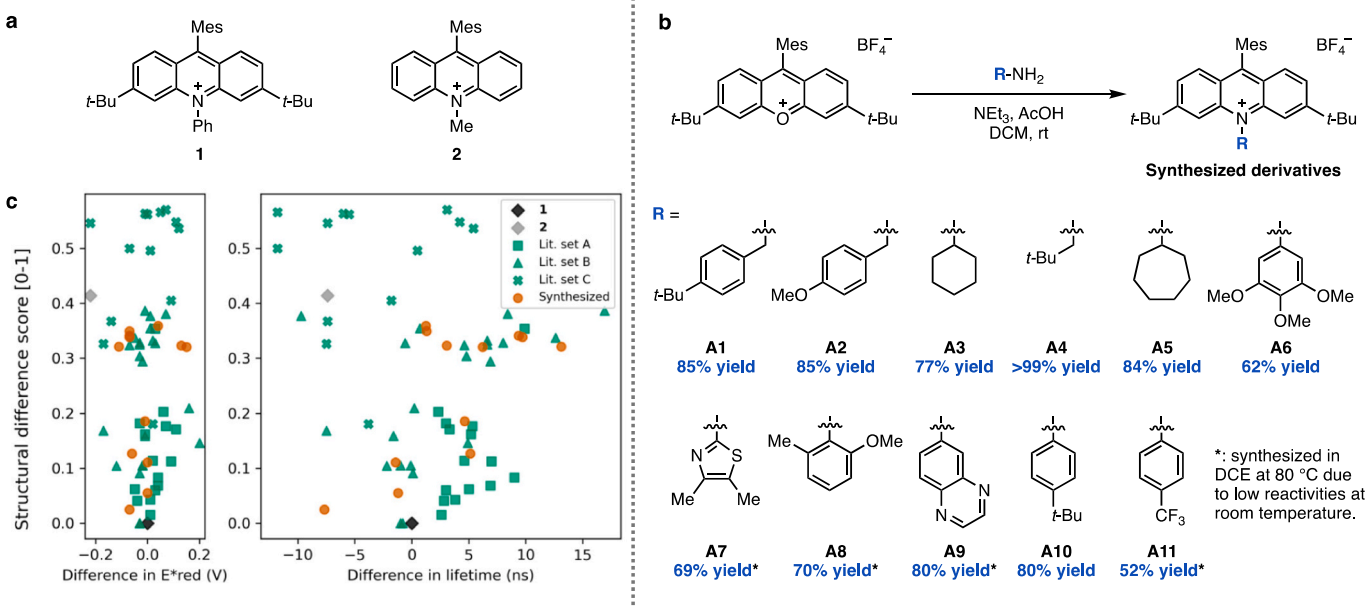

Fig. 1. (a) Two commonly used acridinium photocatalysts (**1**,**2**) in photoredox catalysis. (b) Syntheses and yields of acridinium derivatives with various *N*-substitutions. See Supporting Information for details of experimental conditions. (c) Differences in excited-state reduction potential and excited-state lifetime compared to **1** due to structural differences. Literature set A [2], B [6], C [8] contain known derivatives of acridiniums **1** and **2**.

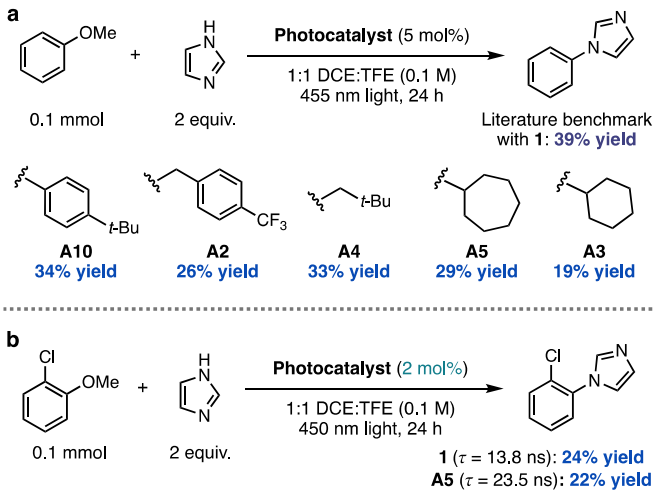

Fig. 2. S_NAr reaction of anisoles with imidazole catalyzed by various acridinium photocatalysts (^1H NMR yield).

halides (E^*_{ox} = −3.36 V) [14]. Mechanistically, the acridine radical (generated from single electron reduction of the excited state acridinium) can be further irradiated to a twisted intramolecular charge transfer (TICT) state that is a potent reductant. This TICT state was proposed to involve the radical anion being localized on the *N*-phenyl ring, highlighting the importance of this substitution.

We decided to screen our library of novel acridinium photocatalysts in the dehalogenation of 4-(trifluoromethyl)phenyl bromide (Fig. 3). Our initial hypothesis was that *N*-aryl acridiniums would be competent in this reaction, while *N*-alkyl acridiniums, being unable to access the TICT state due to the lack of π-conjugation, would give comparatively lower or no yield. As expected, *N*-aryl substituted acridiniums were competent catalysts in this reaction (**A6**, **A8**, **A9**). However, to our surprise, *N*-heterocyclic (**A7**), *N*-benzyl (**A1**, **A2**), and *N*-alkyl (**A3**) photocatalysts were similarly competent in this reaction, with *N*-cyclohexyl acridinium **A3** giving a yield (67 %) within error of that reported for **1** (72 %). The absence of *N*-aryl substituents for **A3** compared to **1** suggests that **A3** is unlikely to access a similar TICT state in the case of **1**. Since the ground-state acridine radical is not sufficient to reduce aryl bromides (the acridine radical of **1** has an E_{ox} of +0.60 V [14]), we hypothesized that a different excited-state in nature might be responsible for the reducing behavior of **A3**. To test this hypothesis, we performed preliminary TD-DFT calculations on the optimized ground state (D_0) geometry of the acridine radicals for all synthesized acridinium catalysts (representative examples of **A3**, **A6**, **A7** shown in Fig. 3), to characterize the nature of electronic transitions for the low-lying excited state (D_1). For *N*-alkyl acridiniums (**A3**, **A4**, **A5**), the electronic transition occurs from π_{core} to π^*_{core} with high orbital overlap, indicating that the D_1 is a locally excited state. The character of D_1 in *N*-aryl acridiniums, however, depends on the aryl substituent. Acridiniums with *electron-rich* aryl substituents (**A1**, **A2**, **A6**, **A8**, **A10**) exhibit electronic transition from π_{core} to an orbital localized on the core and *N*-substituent, suggesting that D_1 is a mixed locally excited and charge-transfer state. Conversely, acridiniums with *electron-poor* aryl substituents (**A7**, **A9**, **A11**), shows electronic transitions from π_{core} to $\pi^*_{N\text{-substituent}}$ and have minimal orbital overlap, indicating that the D_1 is an intramolecular charge-transfer state. Details on the vertical absorption energy and orbitals are available in the Supporting Information. These studies showed that the acridine radicals of acridinium catalysts with various *N*-substituents all have accessible low-lying excited states (albeit different in nature), which may help explain the consistent reduction reactivities observed across catalysts. Further photophysical studies are still needed to elucidate the nature of the photocatalysts in the photoreduction reaction.

Acridiniums in C—H amination

The Doyle lab previously reported a novel cyanoarene photocatalyst, CF_3–4-CzIPN, that can engage in oxidative radical-polar crossover (ORPC) to achieve nucleophilic amination of primary and secondary benzylic C(sp^3)–H bonds [15]. Compared to commonly employed 4-CzIPN (E^*_{red} = +1.43 V), cyanoarenes with a high E^*_{red}, represented by CF_3–4-CzIPN (E^*_{red} = +1.91 V), are most beneficial for this reaction by more readily oxidizing the benzylic radical to a carbocation in the radical-polar crossover step. In addition to an extensive screening of cyanoarenes, we have also previously screened acridinium catalyst **2** (E^*_{red} = +1.88 V) with a high throughput photoreactor set up and found that it is effective in catalyzing the amination reaction [15]. Based on these observations, we hypothesized that more optimal acridinium catalysts could be identified for this reaction.

On the hypothesis that longer excited state lifetimes would also be beneficial to the reactivity of the Ritter amination reaction, we tested *N*-alkyl and *N*-benzyl acridinium catalysts and compared their reactivities with the previously reported best cyanoarene catalyst, CF_3–4-CzIPN, and the commonly used acridinium catalyst **1** (Fig. 4). We started first by

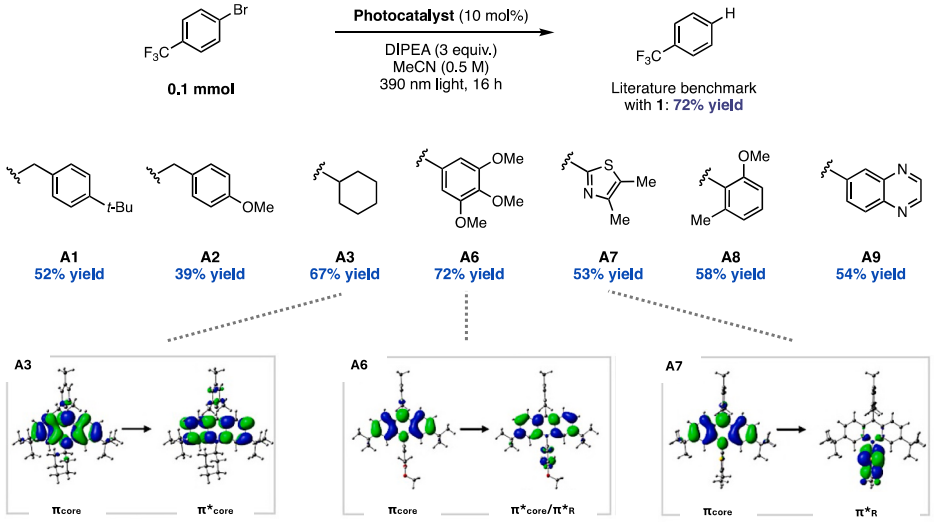

Fig. 3. Reductive debromination reaction catalyzed by various acridinium photocatalysts (^{19}F NMR yield) and TD-DFT studies on the D_0-D_1 transition of acridine radicals for **A3**, **A6**, and **A7**.

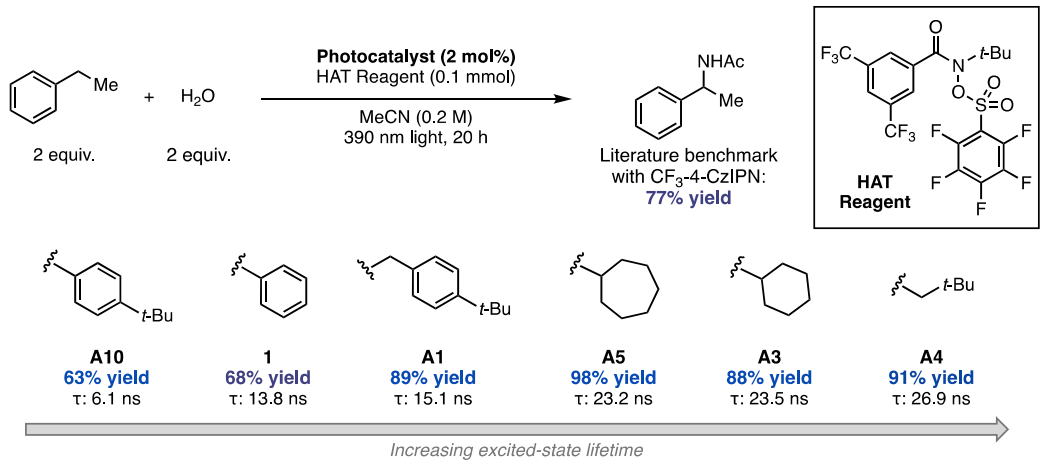

Fig. 4. Nucleophilic C—H amination reaction catalyzed by various acridinium photocatalysts, including two benchmark catalysts CF_3–4-CzIPN and **1** (^{1}H NMR yield).

switching light source from the originally reported 456 nm to a 390 nm Kessil lamp to better match the maximum absorption wavelength of our synthesized acridiniums. Under otherwise identical reaction conditions, we found that *N*-alkyl and *N*-benzyl acridinium catalysts with longer excited-state lifetimes significantly outperformed both **1** (68 % yield) and CF_3–4-CzIPN (77 % yield). Through this optimization we identified catalyst **A5** as most optimal, which provides the desired product in a near-quantitative 98 % yield. As a test of our hypothesis, we also screened *N*-aryl catalyst **A10**, which has a relatively short excited-state lifetime of 6.1 ns and found that the yield decreased significantly.

Following a previously-reported protocol [12], we subjected a solution of catalyst **A5** to an excess of single-electron reductant cobaltocene to generate its reduced acridine species, **A5**$^\bullet$ (Fig. 5a, step 1). Upon addition of this reduced photocatalytic intermediate to a solution of hydrogen atom transfer (HAT) reagent in the absence of light, two signals are observed in the ^{19}F NMR (Fig. 5a, step 3). The right peak indicates residual HAT reagent in the reaction mixture. Notably, formation of a new peak (Fig. 5a, step 3, left) is observed, consistent with formation and fragmentation of the reduced HAT species, generating a new HAT-derived byproduct. Moreover, when this mixture is then irradiated with a 390 nm light source, we observe further conversion of the HAT reagent to its fragmented byproduct (Fig. 5a, step 4). These experiments indicate the photocatalyst is likely undergoing a reductive quenching cycle to generate the reduced acridine radical species, which is then responsible for single-electron transfer (SET) to the HAT reagent, prompting mesolytic fragmentation. Increased conversion of the HAT reagent upon irradiation also suggests that a consecutive photoinduced electron transfer (conPET) mechanism may be in effect, wherein the reduced acridine radical undergoes a second photoexcitation event to promote the subsequent SET to the HAT reagent from its photoexcited state (Fig. 5B). We hypothesize that the increased excited-state lifetimes of the *N*-alkyl and *N*-benzyl acridiniums increases the kinetic efficiency of the SET steps in the catalytic cycle. Moreover, the high conformational flexibility of catalyst **A5** may help to prevent back-electron transfer from the acridine radical intermediate, a common challenge of many ORPC reactions [16,17]. More in-depth mechanistic and computational studies of these novel photocatalysts are needed to elucidate the exact nature of their increased reactivity.

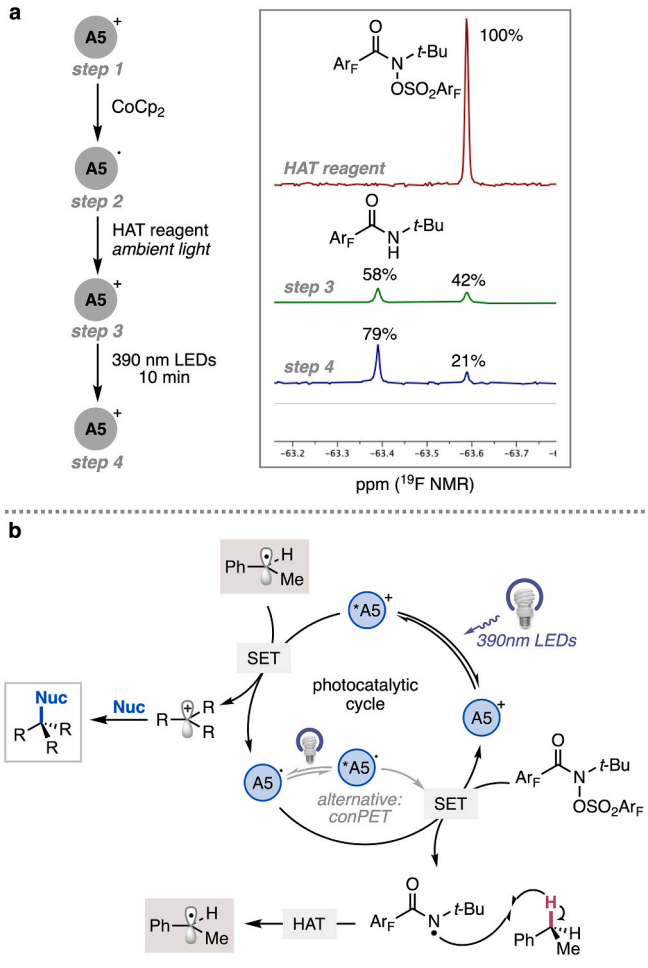

Fig. 5. (a) Mechanistic study on HAT reagent consumption with acridinium photocatalyst **A5**. (b) Proposed catalytic cycle.

Conclusion

We have synthesized a library of acridinium photocatalysts featuring underexplored *N*-(hetero)aryl, *N*-benzyl and *N*-alkyl substitutions. We observed a significant effect of *N*-substitutions on the excited-state lifetimes of acridinium photocatalysts. In addition to being competent catalysts in test reactions featuring various oxidative and reductive pathways, the extended excited-state lifetimes have been shown to improve the reactivities of an ORPC reaction, providing new mechanistic insights and future directions in acridinium photocatalyst design.

CRediT authorship contribution statement

Jason Y. Wang: Writing – review & editing, Writing – original draft, Visualization, Validation, Methodology, Investigation, Conceptualization. **Flora Fan:** Writing – review & editing, Writing – original draft, Visualization, Validation, Methodology, Investigation. **Madeline E. Ruos:** Writing – review & editing, Writing – original draft, Visualization, Validation, Methodology, Investigation. **Leticia Adao Gomes:** Writing – review & editing, Visualization, Methodology, Investigation. **Mimi Lavin:** Methodology, Investigation. **Thomas J. O'Connor:** Methodology, Investigation. **Steven A. Lopez:** Writing – review & editing, Supervision, Project administration, Funding acquisition, Conceptualization. **Abigail G. Doyle:** Writing – review & editing, Supervision, Project administration, Funding acquisition, Conceptualization.

Declaration of competing interest

The authors declare the following financial interests/personal relationships which may be considered as potential competing interests: Abigail Doyle reports financial support was provided by National Science Foundation. Jason Y. Wang reports financial support was provided by University of California Los Angeles. Madeline E. Ruos reports financial support was provided by Bristol Myers Squibb. Steven A. Lopez reports financial support was provided by National Science Foundation. Mimi Lavin reports financial support was provided by National Science Foundation. Flora Fan reports financial support was provided by National Science Foundation. Leticia Adao Gomes reports financial support was provided by National Science Foundation. Thomas J. O'Connor reports financial support was provided by National Science Foundation. If there are other authors, they declare that they have no known competing financial interests or personal relationships that could have appeared to influence the work reported in this paper.

Acknowledgements

Financial support was provided by the United States National Science Foundation (NSF) Office of Advanced Cyberinfrastructure (OAC-2118201). J.Y.W. acknowledges UCLA Dissertation Year Award for financial support. M.E.R. acknowledges support from the BMS Graduate Fellowship in Synthetic Organic Chemistry.

Appendix A. Supplementary data

Supplementary data to this article can be found online at https://doi.org/10.1016/j.tetlet.2025.155546.

Data availability

Data will be made available on request.

References

[1] (a) P.P. Singh, J. Singh, V. Srivastava, Visible-light acridinium-based organophotoredox catalysis in late-stage synthetic applications, RSC Adv. 13 (2023) 10958–10986, https://doi.org/10.1039/d3ra01364b;
(b) A. Tlili, S. Lakhdar, Acridinium salts and Cyanoarenes as powerful Photocatalysts: opportunities in organic synthesis, Angew. Chem. 133 (2021) 19678–19701, https://doi.org/10.1002/ange.202102262.
[2] A. White, L. Wang, D. Nicewicz, Synthesis and characterization of Acridinium dyes for Photoredox catalysis, Synlett 30 (2019) 827–832, https://doi.org/10.1055/s-0037-1611744.
[3] C. Fischer, C. Sparr, Direct transformation of esters into heterocyclic fluorophores, Angew. Chem. Int. Ed. 57 (2018) 2436–2440, https://doi.org/10.1002/anie.201711296.
[4] C. Fischer, C. Sparr, Synthesis of 1,5-bifunctional organolithium reagents by a double directed ortho-metalation: direct transformation of esters into 1,8-dimethoxy-acridinium salts, Tetrahedron 74 (2018) 5486–5493, https://doi.org/10.1016/j.tet.2018.04.060.
[5] V. Hutskalova, C. Sparr, Ad hoc adjustment of Photoredox properties by the late-stage diversification of Acridinium Photocatalysts, Org. Lett. 23 (2021) 5143–5147, https://doi.org/10.1021/acs.orglett.1c01673.
[6] H. Yan, J. Song, S. Zhu, H.-C. Xu, Synthesis of Acridinium Photocatalysts via Site-Selective C–H Alkylation, CCS Chem. 3 (2021) 317–325, https://doi.org/10.31635/ccschem.021.202000743.
[7] A. Gini, M. Uygur, T. Rigotti, J. Alemán, O.G. Mancheño, Novel oxidative Ugi reaction for the synthesis of highly active, visible-light, imide-Acridinium Organophotocatalysts, Chem. Eur. J. 24 (2018) 12509–12514, https://doi.org/10.1002/chem.201802830.
[8] Y.-X. Cao, G. Zhu, Y. Li, N.L. Breton, C. Gourlaouen, S. Choua, J. Boixel, H.-P.J. de Rouville, J.-F. Soulé, Photoinduced Arylation of Acridinium Salts: Tunable Photoredox Catalysts for C–O Bond Cleavage, J. Am. Chem. Soc. 144 (2022) 5902–5909, https://doi.org/10.1021/jacs.1c12961.
[9] D. Bajusz, A. Rácz, K. Héberger, Why is Tanimoto index an appropriate choice for fingerprint-based similarity calculations? J. Chemother. 7 (2015) 20, https://doi.org/10.1186/s13321-015-0069-3.
[10] G. Landrum, Additional Information about the Fingerprints. https://www.rdkit.org/docs/RDKit_Book.html#additional-information-about-the-fingerprints, 2025.
[11] S. Fukuzumi, H. Kotani, K. Ohkubo, S. Ogo, N.V. Tkachenko, H. Lemmetyinen, Electron-transfer state of 9-Mesityl-10-methylacridinium ion with a much longer lifetime and higher energy than that of the natural photosynthetic reaction center, J. Am. Chem. Soc. 126 (2004) 1600–1601, https://doi.org/10.1021/ja038656q.
[12] N.A. Romero, D.A. Nicewicz, Mechanistic insight into the Photoredox catalysis of anti-Markovnikov alkene Hydrofunctionalization reactions, J. Am. Chem. Soc. 136 (2014) 17024–17035, https://doi.org/10.1021/ja506228u.
[13] N.E.S. Tay, D.A. Nicewicz, Cation radical accelerated nucleophilic aromatic substitution via organic Photoredox catalysis, J. Am. Chem. Soc. 139 (2017) 16100–16104, https://doi.org/10.1021/jacs.7b10076.
[14] I.A. MacKenzie, L. Wang, N.P.R. Onuska, O.F. Williams, K. Begam, A.M. Moran, B. D. Dunietz, D.A. Nicewicz, Discovery and characterization of Acridine radical Photoreductants, Nature 580 (2020) 76–80, https://doi.org/10.1038/s41586-020-2131-1.
[15] M.E. Ruos, R.G. Kinney, O.T. Ring, A.G. Doyle, A General Photocatalytic Strategy for Nucleophilic Amination of Primary and Secondary Benzylic C–H Bonds, J. Am. Chem. Soc. 145 (2023) 18487–18496, https://doi.org/10.1021/jacs.3c04912.
[16] S. Fukuzumi, K. Ohkubo, T. Suenobu, Long-lived charge separation and applications in artificial photosynthesis, Acc. Chem. Res. 47 (2014) 1455–1464, https://doi.org/10.1021/ar400200u.
[17] S. Fukuzumi, Y. Lee, W. Nam, Photoredox catalysis of acridinium and quinolinium ion derivatives, Bull. Korean Chem. Soc. 46 (2025) 4–23, https://doi.org/10.1002/bkcs.12922.